Magnetic Resonance Imaging of Vulnerable Carotid Plaques

9

Rohitashwa Sinha, Karol P. Budohoski, Victoria E.L. Young, and Rikin A. Trivedi

1 Introduction

In 1951, C. Miller Fisher first recognized the connection between an occluded carotid artery and cerebral infarction [1]. Since this seminal finding, carotid atherosclerotic disease has been recognized as a thromboembolic source, which may precipitate cerebral ischemic episodes. The present management of carotid atherosclerotic disease is directed at reducing the risk of stroke. This can be achieved surgically, by means of carotid endarterectomy (CEA), however, not without significant perioperative risks involved. Indications for surgical treatment are largely based on investigations that assess the degree of luminal narrowing. The reason behind this is a series of multicentre, randomized controlled trials (RCTs), which have stratified the risk of stroke for symptomatic and asymptomatic patients with various degrees of luminal stenosis undergoing CEA [2–5].

An analysis of the pooled results from the major RCTs: European Carotid Surgery Trial (ECST), North American Symptomatic Carotid Endarterectomy Trial (NASCET), and Veterans' Affairs Trial, demonstrated that a significant benefit can only be achieved in patients with severe stenosis (70–99 %) [6]. The absolute risk reduction (ARR) of ipsilateral stroke within the next 5 years was found to be 16 % [6]. Only a marginal benefit was observed for patients with moderate stenosis (50–69 %) with an ARR of 4.6 % [6]. Furthermore, combined data from the Asymptomatic Carotid Atherosclerosis Study (ACAS) and the Asymptomatic Carotid Surgery Trial (ACST) showed a 5-year stroke risk reduction from 11.5 to 6 %, but only in patients with a significantnarrowing $\geq$70 % [7, 8] It is also worth noting that the benefit was significant only for males aged >75 years [8].

Digital subtraction angiography (DSA) was used to assess the extent of luminal narrowing in the major RCTs for CEA in symptomatic patients [2–5]. However, as an investigation, DSA has low availability, suffers inherent measurement errors with a reported inter-observer variability approaching 10 % [9]. The costs associated with DSA are greater than modern noninvasive vascular imaging such as ultrasonography (US), computed tomography angiography (CTA), or even magnetic resonance angiography (MRA). Furthermore, DSA is time consuming, requires highly skilled interventional radiologists, and has a significant risk burden (0.5–1.3 % permanent neurological complications and 0.4–1.3 % of transient neurological complications) [10–12]. Hence, in asymptomatic patients, ultrasound has been the gold standard first-line investigation in assessing luminal stenosis, despite being undermined by considerable variability in intraobserver measurement readings as well as between interobserver readers [8, 9].

Recently, as the understanding of carotid atherosclerosis pathophysiology has developed, the emphasis on luminal stenosis has diminished, further demonstrating the limitations of DSA and ultrasonography as the first-line investigation modalities. For example, adaptive arterial remodeling mechanisms described first by Glagov et al. [13] in diseased carotid arteries, which allow for large plaques to dilate the outer wall circumference without reducing the lumen may not be detected using DSA alone.

Histological analysis of plaques which were known to have caused cerebrovascular events such as stroke or transient ischemic attack (TIA) have helped to elicit features of the diseased arterial walls which may prove to be more sensitive and accurate markers of disease progression [14, 15]. Recent research using Magnetic Resonance Imaging(MRI) have shown it to be sensitive in identifying features of carotid arterial walls which have been implicated in a significant risk of disease progression [16–18].

R. Sinha (✉) • K.P. Budohoski • V.E.L. Young • R.A. Trivedi
Department of Neurosurgery, Addenbrooke's Hospital, Hills Road, Box 166, CB2 0QQ Cambridge, UK
e-mail: rohitashwa.sinha@addenbrookes.nhs.uk; karol.budohoski@gmail.com; victoria.young@addenbrookes.nhs.uk; rikitrivedi@hotmail.com; rt256@cam.ac.uk; rikin.trivedi@addenbrookes.nhs.uk

L. Saba et al. (eds.), *Multi-Modality Atherosclerosis Imaging and Diagnosis*,
DOI 10.1007/978-1-4614-7425-8_9,

This chapter aims to describe the recent developments in MRI, which make it a promising tool in the evaluation of carotid atherosclerotic disease. The markers of high-risk atherosclerotic plaques visible on MRI and evidence obtained from long-term observational studies will be described.

2 From Luminal Stenosis to Wall Characteristics

Histological characteristics studied in excised carotid specimens from stroke or TIA patients have been fundamental to understanding disease progression in atherosclerosis [19, 20]. Subsequently, the term "vulnerable plaque" was coined, referring to carotid plaques, which exhibit the characteristics that have been commonly found in plaques that were found to have caused cerebrovascular events. Nagahavi et al. proposed the systematic classification of plaques at high risk for thrombosis, rupture, and embolization. Major and minor criteria were proposed. Major criteria include active inflammation within the plaque, a thin fibrous cap (FC) with a large lipid rich necrotic core (LRNC), fibrous cap disruption, as well as severe stenosis. Minor criteria include intraplaque hemorrhage (IPH), expansive remodeling, superficial calcified nodules, yellow coloring on angioscopy, and endothelial dysfunction [21, 22].

Various MRI sequences have been used successfully to depict all of the aforementioned major and minor characteristics within carotid plaques (with the exception of endothelial dysfunction and yellow coloring on angioscopy). Furthermore, studies have ascertained a relationship between MRI signs of "vulnerability" and subsequent risk of stroke and/or TIA. For example, Takaya et al. found a significant correlation between the presence of a thin or ruptured fibrous cap on carotid MRI and ipsilateral ischemic stroke [23]. These characteristics infer a significant risk of future ischemic events for the affected patients irrespective of the extent luminal stenosis. Indeed, several reports indicate that the majority of people with neurological symptoms attributable to ipsilateral internal carotid artery (ICA) atherosclerosis have only moderate ICA stenosis [24].

This shift in emphasis, described above, from hemodynamic compromise caused by luminal stenosis to thromboembolism arising from "vulnerable" atherosclerotic plaques is based on an evolving understanding of the pathophysiology of atherosclerosis. As the disease progresses, an ongoing inflammatory process occurs whereby cholesterol carried by low density lipoproteins (LDL) in the blood is deposited and oxidized in the subendothelial layer of medium and large arteries such as the carotid arteries [25]. Subsequently the LDL become oxidized, attract macrophages, and later also smooth muscle cells. Both these cell types phagocytose the oxidized LDL. The internalized lipids within smooth muscle cells and macrophages interspersed by discrete foci of extruded lipid are histological and, on imaging, seen as the characteristic lipid-rich necrotic core (LRNC). Furthermore, the amount of activated macrophages can be quantitatively assessed and is one of the markers used for imaging the inflammatory process. Both the LRNC and activated macrophages, i.e., inflammation have been classified by Naghavi et al. as major criteria characteristic of vulnerable plaques [21, 22].

The fibrous cap (FC), on the other hand, is formed by the vascular endothelial layer along collagen fibers and matrix glycoproteins which overlie the lipid core [25]. As the intimal lipid core progresses, it incurs local hypoxia leading to necrosis. Hypoxia and necrosis render the delicate neovascular bed of the atherosclerotic plaque prone to the development of intraplaque hemorrhage (IPH) [26–28]. All the above-described processes alongside the increasing biomechanical stress due to deformation of vessel wall and the action of inflammation-induced proteolytic enzymes such as matrix metalloproteinases (MMPs) may lead to the rupture of the fibrous cap and thromboembolism [26, 29–31].

In summary the characteristic stages of the pathophysiology of atherosclerotic plaque formation have been identified and described as the major and minor criteria of plaque vulnerability. The presence of these characteristics increases the risk of subsequent TIA and/or stroke. It has been postulated that the described characteristics may be more sensitive in predicting the risk of TIA and/or stroke than the extent of luminal stenosis. Therefore, the ability to image and monitor their progression is of great clinical importance (Fig. 9.1). Table 9.1 shows the different criteria outlined by Naghavi et al. and the investigative modalities that can be used to assess them [21, 22]. As can be seen at present MRI has the broadest application [32].

3 Magnetic Resonance Imaging

MRI has many advantages, which make it likely to become the investigative modality of choice for imaging carotid disease. It yields images of high spatial resolution, even of soft tissue. Additionally, MRI-derived measurements have been shown to be reproducible and can be used in classifying plaques according to the American Heart Association criteria [33]. It has been shown that imaging plaques in vivo using MRI corresponds well to postoperative histological examination of the excised plaques. It is noninvasive and does not entail patient exposure to ionizing radiation. These particular benefits mean that MRI can safely be used sequentially on the same patient to assess disease progression or response to treatment.

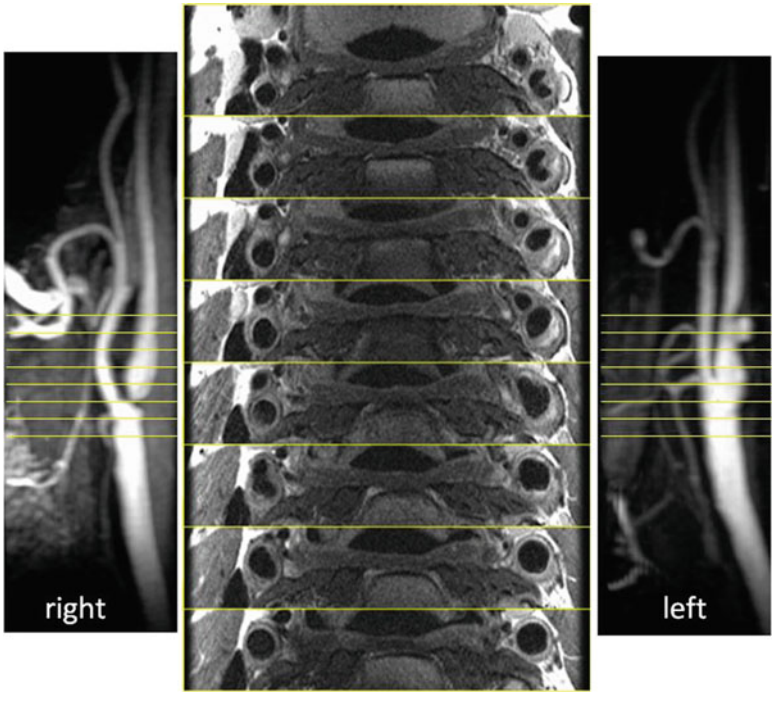

Fig. 9.1 Sequential imaging of bilateral carotid artery stenosis. TOF depicts the area of luminal narrowing. Axial slices depict the full extent of the atherosclerotic process, including expansive remodeling. The atherosclerotic process includes a larger area than seen only by looking at the extent of luminal narrowing. *TOF* time of flight

Table 9.1 Imaging modalities available to assess atherosclerotic carotid plaque characteristics

Plaque characteristic	MRI	CT	US	PET	SPECT	DSA
Active inflammation	✓	X	X	✓	X	X
Thin FC with large LRNC	✓	✓	X	X	X	X
FC disruption	✓	X	X	X	✓	X
Severe stenosis	✓	✓	✓	X	X	✓
Intraplaque hemorrhage	✓	X	X	X	X	X
Expansive remodeling	✓	X	✓	X	X	X
Superficial calcified nodules	✓	✓	X	X	X	X
Yellow coloring on angioscopy	X	X	X	X	X	X
Endothelial dysfunction	✓	X	X	✓	X	X

MRI magnetic resonance imaging, *CT* computed tomography, *US* ultrasonography, *PET positron emission tomography*, *SPECT* single photon, emission computed tomography, *DSA* digital subtraction angiography

The disadvantages of MRI include its costs; it is an expensive technology requiring skilled staff, trained in imaging carotid vessels and using specialist equipment. Furthermore, MRI involves long-image acquisition times and this can pose problems for patients suffering with impaired neurological status, which is often encountered in patients following stroke. MRI is absolutely contraindicated in an important subsection of the patient population with metallic implants, especially those with concomitant coronary atherosclerotic disease who might have implanted cardiac devices. Different techniques using MRI have been used to investigate the key characteristics of "vulnerable" plaques. In the subsequent sections we will outline recent research studies that demonstrate how MRI is being used to investigate each of those characteristics.

4 Fibrous Cap

As discussed earlier, the fibrous cap overlying the lipid core of an atherosclerotic plaque is implicated as the thromboembolic component which, when ruptured, leads to TIA or stroke. Indeed, a number of histological studies have shown that a thin fibrous cap overlying a large lipid-rich necrotic core is a common feature of plaques prone to rupture [15, 21, 34, 35].

High resolution MRI using a 3D "multiple overlapping thin slab angiography" sequence was employed in a study by Hatsukami et al. to assess the feasibility of differentiation types of FC depending on thickness into thin FC, thick FC, and ruptured FC [36]. Their results had an 89 % agreement

with ex vivo histological assessment of the imaged plaques. In a study by Trivedi et al., the authors were able to quantify both fibrous cap and the lipid-rich necrotic core using 2D, blood-suppressed, fast spin echo, T2W MRI sequences with high interobserver agreement [37]. The fibrous cap/lipid-rich necrotic core ratio was introduced. Similar results were later confirmed by other authors, who also found good agreement of the MRI measurements with histological specimens [38]. The specific sequence employed included double inversion recovery, T1W, time of flight, and proton density weighted, which were statistically more accurate than T2-weighted MRI.

These studies demonstrate that fibrous cap identification and measurement can reliably be achieved using specialized high-resolution MRI sequences with reliable comparison to the histological measurements from the same plaques postoperatively. These results suggest that the imaging techniques could be used sequentially to assess disease progression. Additionally, there is wide scope for the morphological parameters visualized with MR to be used for the assessment of therapeutic interventions aimed at stabilizing the plaques and their fibrous caps.

5 Lipid-Rich Necrotic Core

Larger sized LRNC in atherosclerotic plaques have been postulated as inferring greater risk of plaque vulnerability owing to the increased likelihood of hypoxia and necrosis in the LRNC and the increased fragility of neovascularization leading to intraplaque hemorrhage; all of which perpetuate atherosclerotic disease progression. Recent studies have used various different MRI techniques to reliably image and measure the LRNC in vivo.

Echo-planar diffusion-weighted imaging (DWI) was used alongside high resolution MRI to generate apparent diffusion coefficient (ADC) maps in 26 patients with moderate to severe carotid stenosis to distinguish between LRNC and FC. They report a significant difference between the ADC values for the FC and LRNC ($p < 0.0001$) as well as a significant correlation ($p = 0.005$) between ADC values and histology post CEA; lower ADC values matched with heavier lipid staining in the excised specimens.

Underhill et al. [39] used multicontrast MRI in a prospective observational study in 108 asymptomatic individuals with carotid stenosis, imaging at baseline and at 3 years to assess for new ulceration or plaque disruption. Regression analysis revealed that the proportion of wall volume occupied by the LRNC was the strongest predictor of subsequent "surface disruption" and that a new surface disruption was associated with a significant increase in percentage LRNC volume. This particular target step in the pathophysiology may be of special relevance as the point where a stable plaque becomes unstable. The use of high resolution MRI to assess therapy effects on LRNC at this stage is likely to be of great clinical importance.

In a randomized, double-blind, placebo-controlled prospective study over 3 years, [40] used high resolution, multicontrast bilateral carotid MRI scans at baseline and annually in 33 patients to assess the effect of lipid lowering therapy on LRNC volume and as percentage of the diseased wall. They report significant LRNC volume reduction ($p < 0.001$) and significant reduction in LRNC percentage of arterial wall ($p < 0.001$) over 3 years with intensive lipid lowering therapy. The statistically significant reduction in LRNC percentage of the arterial reduction over the first 2 years precedes "plaque regression"; although longer term follow-up would be required to verify whether this change in imaged LRNC will translate into a lower incidence of stroke or TIA in the future.

6 Fibrous Cap Disruption

Histopathological studies have shown that fibrous cap disruption is more frequently found in patients who have suffered from a transient ischemic attack or stroke in the past [26, 41]. Specific assessment of the FC has been shown to be able to detect with good accuracy situations of disrupted fibrous caps, suggestive of plaque rupture (Figs. 9.2 and 9.3). This has been obtained using high resolution MRI with multicontrast protocols [38]. A case series study has demonstrated it possible to use multisequence, cross-sectional MRI with black and bright blood sequences to identify carotid plaques with disrupted fibrous caps [42]. However, the spatial resolution of conventional scanners is approximately 250 μm, which is the dimension of a thin fibrous cap. This demonstrates the existing pitfalls of imaging of carotid atherosclerosis with conventional MRI scanners.

7 Intraplaque Hemorrhage

Fragile neovascularization in the inflammation-ridden atherosclerotic plaque is prone to hemorrhage. Current thinking suggests that hemorrhage within the atherosclerotic plaque perpetuates the inflammatory processes and induces further necrosis. All these increase the risk of ipsilateral stroke.

As with imaging of the lipid-rich necrotic core, a variety of recent studies have used different MRI techniques to successfully investigate intraplaque hemorrhage in carotid atherosclerotic lesions (Fig. 9.4).

One study compared contrast-enhanced MR angiography (CE-MRA) with time-of-flight (TOF) MRA sequences in 15 patients and validated their accuracy with histological

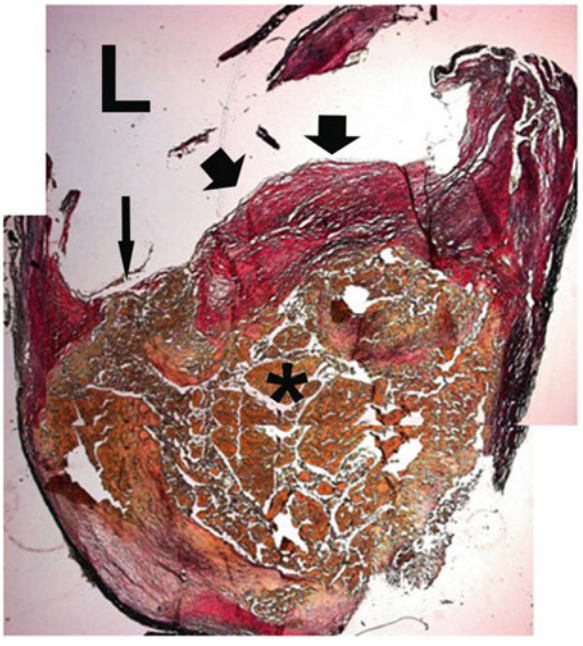

Fig. 9.2 Histological specimen of a atherosclerotic carotid artery. A thin fibrous cap is seen (*short arrow*), with a rupture at one of the edges (*long arrow*). Below the fibrous cap the lipid-rich necrotic core can be seen (*asterisk*). L signifies arterial lumen

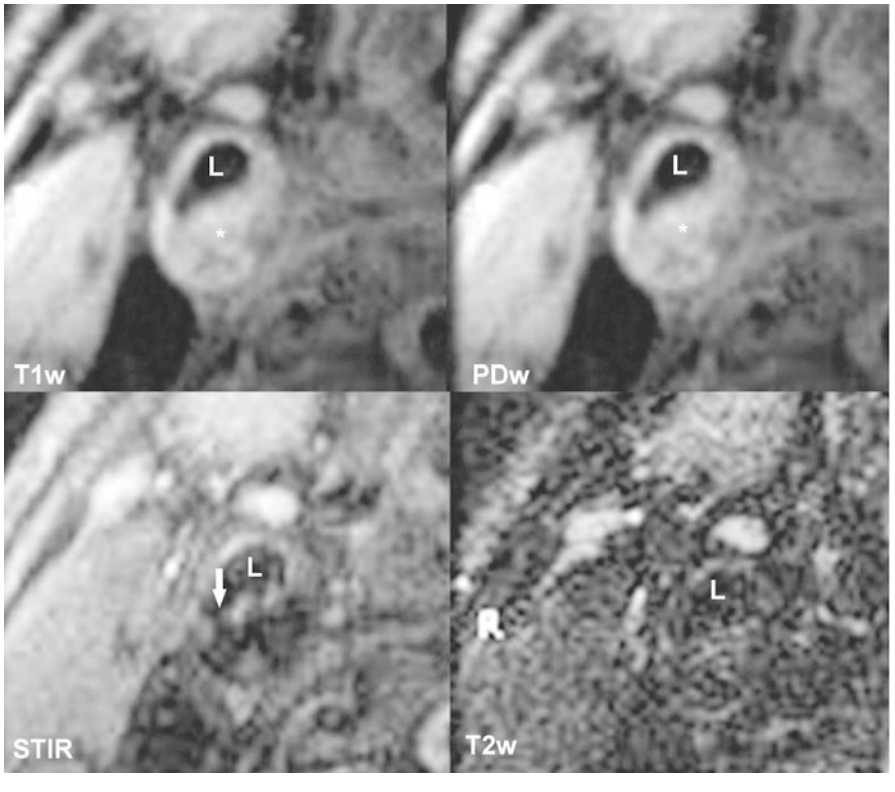

Fig. 9.3 T1w, PDw, STIR, T2w images of the same plaque as in Fig. 9.2. Ruptured fibrous cap is visible in the STIR sequence (*long arrow*). L signifies arterial lumen, *asterisk* signifies the lipid-rich necrotic core. *T1w* T1-weighted sequence, *PDw* proton density-weighted sequence, *STIR* short T1 inversion recover sequence, *T2w* T2-weighted sequence

findings from the ex vivo post-CEA plaque specimens. They report a 94 % accuracy with CE-MRA over 84 % using TOF sequences, with excellent intra and interobserver agreement [43].

Improvements in the technique for imaging intraplaque hemorrhage have been made. One study reported the use of a novel technique to improve on IPH identification, which has previously relied on methemoglobin detection with T1-weighted sequences and blood suppression [44]. They report their novel technique "slab-selective phase-sensitive inversion-recovery" (SPI) optimizes IPH detection and is validated against histology, with significantly

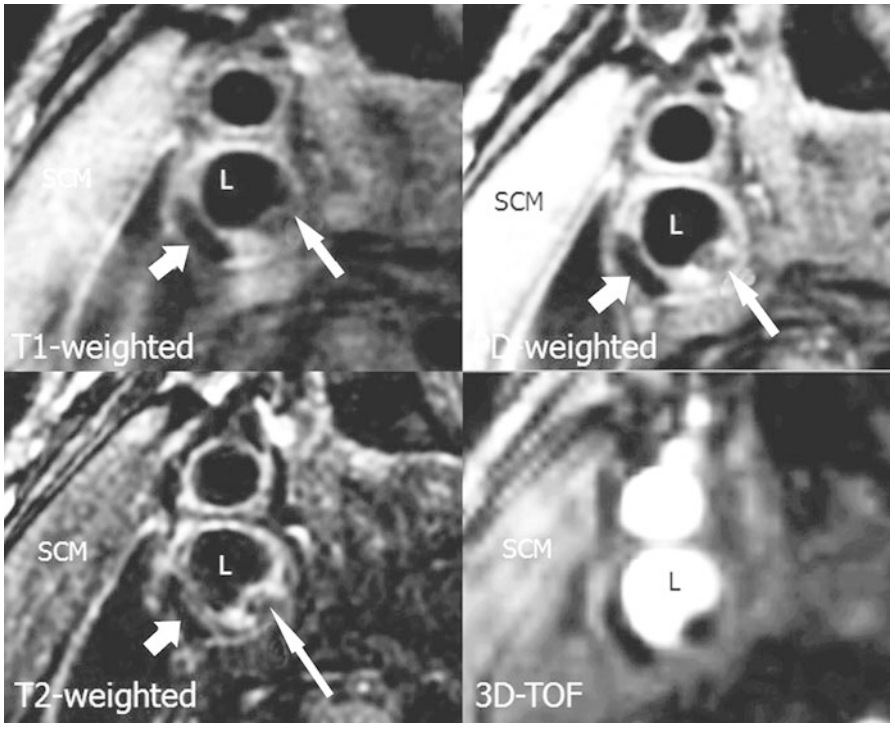

Fig. 9.4 MRI image with T1w, PDw, T2w, and 3D-TOF demonstrating thrombus within a carotid artery plaque (*short arrow*). Additionally thrombus with partial calcifications is seen in adjacent area (*long arrow*). L indicates arterial lumen. *T1w* T1-weighted sequence, *PDw* proton density-weighted sequence, *T2w* T2-weighted sequence, *3D-TOF* 3-dimensional time of flight

improved intraplaque hemorrhage-wall contrast-to-noise ratio ($p < 0.01$) and blood suppression efficiency ($p < 0.01$) when compared with recently used 3D rapid acquisition gradient echo sequences.

8 Wall Thickness

As the focus has shifted from vessel lumen stenosis to the arterial vessel wall, the relationship between the overall wall thickness and the percentage of the wall occupied by the LNRC has also been emphasized as a risk-stratifying characteristic. In the Carotid Atherosclerosis Score (CAS) [39], maximal vessel wall thickness (VWT) and the percentage of the wall occupied by the LRNC were the strongest predictors of FC disruption and IPH.

VWT and vessel wall area (VWA) have been used as surrogate markers of expansive remodeling, whereby the plaque progression occurs by enlarging the vessel wall outwards rather than encroaching on the lumen size. Black-blood fast spin-echo sequences were used in a prospective clinical trial of the effects of 12, 18, and 24 months of simvastatin lipid lowering therapy on VWT and VWA [45, 46]. Changes in both VWT and VWA at all the predefined times were statistically significant; the reduction in VWA size at 24 months compared to baseline ($p < 0.0001$) and VWT ($p < 0.001$). This feasibility study showed that MRI can be used in clinical trials to evaluate treatment efficacy, by means of assessing the change in wall characteristics rather than the degree of lumen stenosis in a longitudinal manner.

9 Inflammation

The inflammatory process within the plaque itself plays a major role in all aspects of atherosclerosis, i.e., plaque initiation, plaque progression, and plaque rupture. Systemic markers of inflammation, such as C-reactive protein (CRP) have been correlated with the cardiovascular events due to atherosclerotic disease [47]. Furthermore, inflammation has become a target of new therapies for atherosclerosis. While the exact mechanisms of inflammation related to atherosclerosis are beyond the scope of this chapter, macrophage infiltration of the plaque and neovascularization are of the plaque are two aspects, which have been recognized as potential markers of plaque vulnerability. MRI using a specific, macrophage-directed contrast agent, such as ultrasmall superparamagnetic iron oxide (USPIO) and dynamic contrast-enhanced MRI (DCE-MRI) using traditional gadolinium-based contrast agents have been used [48–51].

10 USPIO-Enhanced MRI and Macrophage Content

Ultrasmall superparamagnetic iron oxide (USPIO) is a non-gadolinium-based contrast agent that has been shown to be useful in MRI. The USPIO particle consists of a microcrystalline magnetite core, within dextran coating. Typically the diameter of USPIO is around 30 nm [52]. The particles are

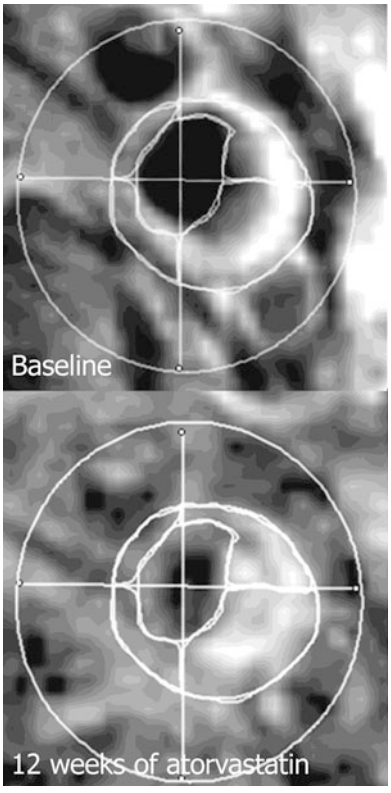

Fig. 9.5 USPIO-enhanced MRI at baseline and after 12 weeks of atorvastatin therapy. Note the increased enhancement in the *right upper* and *lower quadrant* signifies a lower USPIO accumulation, thus, reduced inflammatory process

absorbed by the reticuloendothelial system (RES) of the liver and spleen and are subsequently nonselectively absorbed by activated macrophages. Activated macrophages accumulate in areas of active inflammation, such as atherosclerotic plaques, but not only, and thus can be visualized using MRI [53, 54].

The effect of USPIO on MRI imaging has been described by Bulte et al. [55]. Briefly, USPIO particles create a large dipolar magnetic field, which acts on water molecules thus reducing the T2 relaxation times. USPIO acts as a negative contrast is on T2-weighted (T2W) sequences [55] (Fig. 9.5).

The uptake of USPIO particles by macrophages has been demonstrated in experimental studies [53] and later confirmed in plaques from carotid arteries of humans [49, 54, 56, 57]. Later, Trivedi et al. described the temporal relationship of the magnitude of signal loss following USPIO administration, establishing an optimal window for imaging between 24 and 36 h following administration of contrasting medium [57].

Interestingly no relationship between USPIO uptake of carotid plaques and luminal narrowing was demonstrated [58]. On the other hand, a relationship between inflammation as seen using USPIO-enhanced MRI and biomechanical stress has been demonstrated [59]. These results suggest the degree of inflammation may be an independent factor in determining the risk of plaque progression and subsequent risk of cerebrovascular events. Such findings prompted the question whether inflammation can be used as a surrogate end-point in clinical trials aimed at medical reduction of plaque burden.

The first use of USPIO-enhanced MRI for this purpose was published by Tang et al. in the ATHEROMA trial [60]. Forty-seven patients with asymptomatic carotid atherosclerosis (≥40 % stenosis) were randomized into two groups of high-dose (80 mg/day) and low-dose (10 mg/day) atorvastatin. While a significant reduction in USPIO uptake was demonstrated in the high-dose atorvastatin group as early as 6 weeks after initiation of treatment, no such effect was noted in the low-dose group. Previously interventional studies aimed at reducing plaque burden have focused on morphological characteristics [15, 45, 46, 61, 62]. Similarly, these studies showed that improvements in gross morphological parameters such as vessel wall thickens and vessel wall area, precede changes in luminal stenosis. However, the earliest changes were visible after 12 months of treatment. In contrast using USPIO-enhanced MRI quantifiable changes were demonstrated as early as 6 weeks following start of therapy. These results demonstrate the potential of novel imaging techniques in the rapid assessment of plaque vulnerability and therefore patient risk stratification. It needs to be noted that only patients with baseline uptake of USPIO particles were included in the ATHEROMA study, potentially limiting the generalization of the results to a wider population [60]. However, the potential of imaging inflammation has been demonstrated giving incentive for further development in this area.

11 Dynamic Contrast-Enhanced MRI

Gadolinium-based contrast media are used for their T1-shortening ability. The accumulation of the contrast causes T1 hyperintensity. With the implementation of gadolinium chelates, investigation of the late-phase enhancement is possible. Late enhancement is used as a surrogate marker of contrast diffusion into the extracellular compartment. In order to visualize the vessel wall, sufficient suppression of the blood signal is essential, hence the choice of image acquisition is essential when DCE-MRI is used. Commonly black blood T1W sequences with either double inversion-recovery (DIR) [63] or even, quadruple inversion-recovery (QIR) are used [64].

Studies have shown that the extent of microvasculature within a plaque corresponds to the risk of intraplaque hemorrhage and subsequent rupture [30, 65]. Neovascularization

is induced by the chronic inflammatory process occurring in the plaque. Dynamic contrast-enhanced MRI (DCE-MRI), a method, which was originally developed for in neuro-oncology to determine the extent of tumor neovascularization, has been recently implemented in the study of carotid atherosclerosis. The main advantage of this method is that it can utilize routinely available contrasting media [66]. The first human observation of enhancement of atherosclerotic plaques was observed by Aoki et al. [67]. However, two separate aspects of plaque enhancement have been noted. In the first reports a hyperintense rim surrounding the diseased vessel was reported [67]. This was thought to represent vasa vasorum in the adventitia of the artery. However, direct enhancement within the plaque, in particular the FC was also noted [51, 68].

Kinetic modeling plays the role in the image analysis today [48, 69, 70]. Two parameters which are considered for analysis are fractional plasma volume (V_p) and transfer constant of the contrast agent (K^{trans}) and represent the two compartments: intravascular space and extravascular, extracellular space. V_p is thought to represent the actual microvascular volume [48]. It was found to be a good marker of plaque neovasculature when compared with histology ($r = 0.68$, $p < 0.001$) [48, 70]. K^{trans}, on the other hand, is used to estimate the permeability of the microvasculature. Interestingly, it was K^{trans} which was found to correlate with macrophage content within the plaque suggesting that there may be distinct features of the neovascular bed which are associated with inflammation [48].

One major pitfall of MRI-contrasting agents is the non-specific enhancement, which may unfavorably alter results. MRI contrasting media development is currently concentrating on designing new markers, which would bind to specific targets in the atherogenic process. This progress is being done on the molecular and cellular level. Contrast media that bind to lipid [71, 72], thrombus [73], specific inflammatory mediators [74–76], apoptotic cells [77], and proteolytic enzymes, which could contribute to plaque destabilization [77], are currently under investigation and have the potential to obtain similar binding specificity as the one found in nuclear medicine.

12 Biomechanical Stress Modeling

The biomechanical forces acting on diseased arterial walls with atherosclerotic plaques prone to rupture have also been successfully modeled using MRI techniques [78]. As the inflamed endothelial layers are subject to biomechanical stress from hyperkinetic and turbulent blood flow, the structural integrity becomes progressively compromised which may lead to plaque rupture [78]. Such stresses can be measured using finite elements analysis (FEA) [79].

Trivedi et al. have used MRI-derived 2D geometrical arterial models to perform FEA to predict the differences in plaque tensile stress between symptomatic and asymptomatic patients with carotid atherosclerosis [80]. They reported a substantial difference in principal tensile stress calculated between the two groups.

A recent study used MRI-derived FEA, in a series of 45 patients with carotid atherosclerosis, to demonstrate that plaques with IPH had significantly higher stress than non-hemorrhagic plaques ($p = 0.003$) [81]. Furthermore, biomechanical stress has been used to determine the effect of lipid lowering therapies on carotid atherosclerotic plaques [82]. A reduction in arterial wall strain following aggressive lipid lowering therapy was determined using MR-based modeling. Maximum arterial wall strain at 12 weeks of treatment was significantly lower in the high dose Atorvastatin (80 mg) patient group versus the low dose (10 mg) group [82].

13 Recent Trends and Future Directions

The described studies illustrating how different MR techniques have been used to evaluate the individual "high risk" components of atherosclerotic carotid plaques are by no means the only research employing MR for this purpose. MRI-derived measurements have been shown to be reproducible and that they can be used in classifying plaques according to the American Heart Association criteria [33]. Furthermore, it has been shown that imaging plaques in vivo using MRI corresponds well to postoperative histological examination of the excised plaques [34, 51]. The efficacy and feasibility of MRI in imaging vulnerable carotid plaques has been repeatedly demonstrated [32, 33, 37, 39, 42, 48, 83]. MRI is increasingly being adopted as the imaging tool in prospective studies. It has been successfully used in longitudinal studies [46, 61, 84], as well as clinical intervention trials [60, 85, 86] (Table 9.2).

A recent study by Bianda et al. [84] used high spatial resolution MRI to quantify the progression of atherosclerotic disease in 30 patients over 2 years, looking at both their carotid and femoral arteries. Crucially, patients' medication regimens remained stable throughout the whole study period. The authors were able to quantitatively measure the changes in lumen area, total vessel area, and vessel wall area at baseline and at 1 and 2-year follow-up. Interestingly, differences in plaque progression were found between femoral artery plaques and carotid artery plaques. During the 2 years observation period, the authors demonstrated disease progression (as demonstrated by an increase in vessel wall area), despite standard medical therapy with good compliance. However, only in carotid arteries the increase in plaque size was accompanied by a significant decrease in lumen area. Despite methodological limitations, (inclusion criteria required

Table 9.2 Summary of recent longitudinal studies and clinical trials using MRI measures as primary or secondary end points

Author	Design	*n*	Intervention	Time	Imaging	Results
Corti et al. [45, 46]	Long.	18	Simvastatin	24 months	DIR, FSE PDw, T2w	VWA: decrease of 15 % and 18 % at 12 and 24 months; VWT: decrease of 11 % and 19 % at 12 and 24 months; LA: increase of 5 % at 24 months
Lima (2004) [87]	RCT	27	20 vs. 80 mg/day simvastatin	6 months	DIR, FSE PDw, T2w	PV: decrease of 12 % from baseline; PA: decrease of 12 % from baseline; no difference between groups
Corti et al. [61]	RCT	51	20 vs. 80 mg/day simvastatin	24 months	DIR, FSE PDw, T2w	VWA: decrease of 14 % and 18 % at 12 and 24 months, respectively; VWT: decrease of 10 % and 17 % at 12 and 24 months, respectively; LA: increase of 4 % and 5 % at 12 and 24 months, respectively; no differences between groups
Underhil et al. [62]	RCT	43	5 vs. 40/80 mg/day rosuvastatin	24 months	DIR, FSE T1w, PDw, T2w, 3D TOF	LV, WV, NWI: no changes neither between groups nor between baseline and 24 months; %LRNC: decrease of 37.0 % in high-dose group, no change in low-dose group
Tang et al. [60]	RCT	47	10 vs. 80 mg/day atorvastatin	12 weeks	USPIO-enhanced	ΔSI: 0.203 (95 % CI: 0.065, 0.198) reduction from baseline at 6 weeks (high-dose); difference of 0.240 (95 % CI: 0.134, 0.347) between groups at 12 weeks
Fayad et al. [85]	RCT	130	Dalcetrapib vs. placebo	48 months	TOF, DCE	Reduction in VA in dalcetrapib vs. placebo after 24 months; absolute change from baseline relative to placebo: -4.01 mm^2 (90 % CI: -7.23 to -0.80; nominal $p = 0.04$)
Bianda et al. [84]	Long.	30	Standard medical management	48 months	DIR, FSE T1w, PDw, T2w, 3D TOF	LA decreased (-3.19 %/year, $p = 0.018$); VWA increased ($+3.83$ %/year, $p = 0.019$)

DIR double inversion recovery, *FSE* fast spin echo, *T1w* T1 weighted, *T2w* T2 weighted, *PDw* proton density weighted, *TOF* time of flight, *DCE* dynamic contrast enhanced, *Long* longitudinal, *USPIO* ultrasmall superparamagnetic iron oxide, *VWT* vessels wall thickness, *VWA* vessel wall area, *LA* lumen area, *PA* plaque area, *PV* plaque volume, *ΔSI* signal intensity change, *SUV* standardized uptake value

<70 % stenosis in the carotid arteries while all grades of stenosis in the femoral arteries were permitted) the study successfully demonstrated the sensitivity and usefulness of MRI in monitoring atherosclerosis disease progression.

The recently published dal-PLAQUE (Safety and efficacy of dalcetrapib on atherosclerotic disease using novel noninvasive multimodality imaging) study [85], was designed to assess the efficacy of Dalcetrapib (a cholesterol ester transfer protein inhibitor) on atherosclerotic disease. Simultaneous MR and PET imaging was undertaken to assess the primary endpoints at 2 years from baseline. MRI was used to assess structural changes in carotid arterial walls (total vessel area, wall area, wall thickness, and normalized wall index). Patients treated with Dalcetrapib not only did not demonstrate progression of carotid plaques but were also found to have significant reductions in plaque burden as compared with placebo. Together with the atorvastatin therapy: effects on reduction of macrophage activity (ATHEROMA) study [60], dal-PLAQUE have been the first interventional clinical trials in the field of carotid atherosclerosis to use noninvasive imaging as primary endpoints. The authors of dal-PLAQUE conclude by stating that the imaged vascular endpoints will need even further and longer term clinical validation of the safety of Dalcetrapib on cardiovascular morbidity and mortality. These results are to be published in the "dal-OUTCOMES" trial.

Another study used MR to quantitatively detect changes in the size and composition of carotid plaques following cilostazol therapy; an antiplatelet agent [88]. They prospectively imaged 16 patients at baseline and at 6 months, using methodology where analysis of atherosclerotic plaques is performed calculating a contrast ratio between the imaged plaque and the sternocleidomastoid muscle. They also analyzed the intraplaque components and their relative size in percentage of total area (i.e., fibrous tissue, lipid/necrosis, and hemorrhage components). It was shown that the fibrous component increased significantly, while the lipid and hemorrhagic components decreased. Unfortunately, due to factors such as the small sample size and the lack of a control group, these findings cannot reliably be attributed to the therapeutic effects of Cilostazol.

Aside from MR evaluation of plaque morphology in vivo clinical studies, a recent longitudinal study simultaneously assessed the relationship of biomechanical structural stresses on the atherosclerotic plaques of previously symptomatic patients with a past history of a recent (<1 month) transient ischemic attack or a minor, nondisabling stroke in the last month [89]. They followed up patients clinically from a baseline MR assessment for up to 2 years or until they suffered a cerebrovascular event in the territory of the previously imaged carotid artery. The baseline MR imaging underwent "finite elements analysis" to integrate information regarding plaque morphology, material properties of the plaque constituents, and patient-specific blood pressure during the computational simulations. The additional information provided by the stress factors, the authors' state, give a much more comprehensive assessment of plaque vulnerability compared with plaque morphology alone. This is especially useful in the subset of patients in whom there may be a history of neurological symptoms but who have a moderate degree of luminal stenosis. They report that plaques with hemorrhage or fibrous cap rupture had six to seven times greater likelihood of being associated with subsequent ischemic events, high structural stresses were seen to increase the chance of subsequent events by 13 times.

Further adaptation of currently used MR protocols in clinical studies look likely to refine the use of MR to evaluate prognostic risk, therapeutic effects, and the natural pathophysiology of carotid atherosclerosis with even greater reliability than currently seen. Future work incorporating stress analysis and plaque morphology with bigger patient sample sizes may well prove to be of vital importance in stratifying risk more accurately than the cumbersome luminal stenosis assessment by ultrasound. Such dynamic evaluation of vulnerable plaques could indicate another group of patients who may benefit from CEA, such as those who currently have mild to moderate degrees of luminal stenosis but have "high risk" plaque morphological characteristics and high stresses exerted on the plaques. Alternatively, using 3D volumetric MR measurements of vulnerable plaques, as suggested by [88] and Bianda et al. [84], may be another route for development of MR in imaging carotid atherosclerosis.

14 Conclusions

Current research is unanimous in its shift of focus from the stenosed lumens of atherosclerotic carotid arteries to the arterial wall characteristics that signify earlier phases in the pathophysiology of atherosclerotic plaque progression than the relatively late feature of luminal stenosis. Morphological features such as the vessel wall thickness, lipid-rich necrotic core, intraplaque hemorrhage, fibrous cap size, and disruption as well as biomechanical stress can all be reliably assessed with a variety of high-resolution MRI techniques which are well validated against histological measurements from the same plaques ex vivo. Even inflammatory characteristics of the wall, such as neovascularization and macrophage infiltration in the plaque can be visualized with the use of gadolinium contrast and ultrasmall superparamagnetic iron oxide-enhanced MRI.

As a result, the crude and outdated assessments of degree of lumen stenosis by modalities such as digital subtraction angiography and ultrasound have largely been replaced with MRI as the modality of choice to investigate further details in the pathophysiology of carotid atherosclerosis, to establish patient risk stratification on more sensitive characteristics, and to assess the efficacy of therapeutic interventions at a much earlier stage than previously possible. With newer molecular contrast media being developed to depict in even more detail the full functional history of carotid atherosclerotic plaques, MRI as a modality seems to be indispensable in the future management of this disease.

References

1. Fisher M (1951) Occlusion of the internal carotid artery. AMA Arch Neurol Psychiatry 65:346–377
2. Barnett HJ, Taylor DW, Eliasziw M, Fox AJ, Ferguson GG, Haynes RB, Rankin RN, Clagett GP, Hachinski VC, Sackett DL, Thorpe KE, Meldrum HE, Spence JD (1998) Benefit of carotid endarterectomy in patients with symptomatic moderate or severe stenosis. North American Symptomatic Carotid Endarterectomy Trial Collaborators. N Engl J Med 339:1415–1425
3. Hobson RW 2nd, Weiss DG, Fields WS, Goldstone J, Moore WS, Towne JB, Wright CB (1993) Efficacy of carotid endarterectomy for asymptomatic carotid stenosis. The Veterans Affairs Cooperative Study Group. N Engl J Med 328:221–227
4. Mayberg MR, Wilson SE, Yatsu F, Weiss DG, Messina L, Hershey LA, Colling C, Eskridge J, Deykin D, Winn HR (1991) Carotid endarterectomy and prevention of cerebral ischemia in symptomatic carotid stenosis. Veterans Affairs Cooperative Studies Program 309 Trialist Group. JAMA 266:3289–3294
5. (1998) Randomised trial of endarterectomy for recently symptomatic carotid stenosis: final results of the MRC European Carotid Surgery Trial (ECST). Lancet 351:1379–1387
6. Rothwell PM, Eliasziw M, Gutnikov SA, Fox AJ, Taylor DW, Mayberg MR, Warlow CP, Barnett HJ (2003) Analysis of pooled data from the randomised controlled trials of endarterectomy for symptomatic carotid stenosis. Lancet 361:107–116
7. (1995) Endarterectomy for asymptomatic carotid artery stenosis. Executive Committee for the Asymptomatic Carotid Atherosclerosis Study. JAMA 273:1421–1428
8. Halliday A, Mansfield A, Marro J, Peto C, Peto R, Potter J, Thomas D (2004) Prevention of disabling and fatal strokes by successful carotid endarterectomy in patients without recent neurological symptoms: randomised controlled trial. Lancet 363:1491–1502
9. Young GR, Humphrey PR, Shaw MD, Nixon TE, Smith ET (1994) Comparison of magnetic resonance angiography, duplex ultrasound, and digital subtraction angiography in assessment of extracranial internal carotid artery stenosis. J Neurol Neurosurg Psychiatry 57:1466–1478

10. Hankey GJ, Warlow CP, Molyneux AJ (1990) Complications of cerebral angiography for patients with mild carotid territory ischaemia being considered for carotid endarterectomy. J Neurol Neurosurg Psychiatry 53:542–548
11. Johnston DC, Chapman KM, Goldstein LB (2001) Low rate of complications of cerebral angiography in routine clinical practice. Neurology 57:2012–2014
12. Willinsky RA, Taylor SM, TerBrugge K, Farb RI, Tomlinson G, Montanera W (2003) Neurologic complications of cerebral angiography: prospective analysis of 2,899 procedures and review of the literature. Radiology 227:522–528
13. Glagov S, Weisenberg E, Zarins CK, Stankunavicius R, Kolettis GJ (1987) Compensatory enlargement of human atherosclerotic coronary arteries. N Engl J Med 316:1371–1375
14. Stary HC, Chandler AB, Glagov S, Guyton JR, Insull W Jr, Rosenfeld ME, Schaffer SA, Schwartz CJ, Wagner WD, Wissler RW (1994) A definition of initial, fatty streak, and intermediate lesions of atherosclerosis. A report from the Committee on Vascular Lesions of the Council on Arteriosclerosis, American Heart Association. Circulation 89:2462–2478
15. Stary HC, Chandler AB, Dinsmore RE, Fuster V, Glagov S, Insull W Jr, Rosenfeld ME, Schwartz CJ, Wagner WD, Wissler RW (1995) A definition of advanced types of atherosclerotic lesions and a histological classification of atherosclerosis. A report from the Committee on Vascular Lesions of the Council on Arteriosclerosis, American Heart Association. Circulation 92:1355–1374
16. Saam T, Hatsukami TS, Takaya N, Chu B, Underhill H, Kerwin WS, Cai J, Ferguson MS, Yuan C (2007) The vulnerable, or high-risk, atherosclerotic plaque: noninvasive MR imaging for characterization and assessment. Radiology 244:64–77
17. Stemme S, Faber B, Holm J, Wiklund O, Witztum JL, Hansson GK (1995) T lymphocytes from human atherosclerotic plaques recognize oxidized low density lipoprotein. Proc Natl Acad Sci USA 92:3893–3897
18. Yuan C, Zhang SX, Polissar NL, Echelard D, Ortiz G, Davis JW, Ellington E, Ferguson MS, Hatsukami TS (2002) Identification of fibrous cap rupture with magnetic resonance imaging is highly associated with recent transient ischemic attack or stroke. Circulation 105:181–185
19. Imparato AM, Riles TS, Gorstein F (1979) The carotid bifurcation plaque: pathologic findings associated with cerebral ischemia. Stroke 10:238–245
20. Moore WS, Hall AD (1968) Ulcerated atheroma of the carotid artery. A cause of transient cerebral ischemia. Am J Surg 116:237–242
21. Naghavi M, Libby P, Falk E, Casscells SW, Litovsky S, Rumberger J, Badimon JJ, Stefanadis C, Moreno P, Pasterkamp G, Fayad Z, Stone PH, Waxman S, Raggi P, Madjid M, Zarrabi A, Burke A, Yuan C, Fitzgerald PJ, Siscovick DS, de Korte CL, Aikawa M, Airaksinen KE, Assmann G, Becker CR, Chesebro JH, Farb A, Galis ZS, Jackson C, Jang IK, Koenig W, Lodder RA, March K, Demirovic J, Navab M, Priori SG, Rekhter MD, Bahr R, Grundy SM, Mehran R, Colombo A, Boerwinkle E, Ballantyne C, Insull W Jr, Schwartz RS, Vogel R, Serruys PW, Hansson GK, Faxon DP, Kaul S, Drexler H, Greenland P, Muller JE, Virmani R, Ridker PM, Zipes DP, Shah PK, Willerson JT (2003) From vulnerable plaque to vulnerable patient: a call for new definitions and risk assessment strategies: Part II. Circulation 108:1772–1778
22. Naghavi M, Libby P, Falk E, Casscells SW, Litovsky S, Rumberger J, Badimon JJ, Stefanadis C, Moreno P, Pasterkamp G, Fayad Z, Stone PH, Waxman S, Raggi P, Madjid M, Zarrabi A, Burke A, Yuan C, Fitzgerald PJ, Siscovick DS, de Korte CL, Aikawa M, Juhani Airaksinen KE, Assmann G, Becker CR, Chesebro JH, Farb A, Galis ZS, Jackson C, Jang IK, Koenig W, Lodder RA, March K, Demirovic J, Navab M, Priori SG, Rekhter MD, Bahr R, Grundy SM, Mehran R, Colombo A, Boerwinkle E, Ballantyne C, Insull W Jr, Schwartz RS, Vogel R, Serruys PW, Hansson GK, Faxon DP, Kaul S, Drexler H, Greenland P, Muller JE, Virmani R, Ridker PM, Zipes DP, Shah PK, Willerson JT (2003) From vulnerable plaque to vulnerable patient: a call for new definitions and risk assessment strategies: Part I. Circulation 108:1664–1672
23. Takaya N, Yuan C, Chu B, Saam T, Underhill H, Cai J, Tran N, Polissar NL, Isaac C, Ferguson MS, Garden GA, Cramer SC, Maravilla KR, Hashimoto B, Hatsukami TS (2006) Association between carotid plaque characteristics and subsequent ischemic cerebrovascular events: a prospective assessment with MRI – initial results. Stroke 37:818–823
24. Brown PB, Zwiebel WJ, Call GK (1989) Degree of cervical carotid artery stenosis and hemispheric stroke: duplex US findings. Radiology 170:541–543
25. Berliner JA, Navab M, Fogelman AM, Frank JS, Demer LL, Edwards PA, Watson AD, Lusis AJ (1995) Atherosclerosis: basic mechanisms. Oxidation, inflammation, and genetics. Circulation 91:2488–2496
26. Fisher M, Paganini-Hill A, Martin A, Cosgrove M, Toole JF, Barnett HJ, Norris J (2005) Carotid plaque pathology: thrombosis, ulceration, and stroke pathogenesis. Stroke 36:253–257
27. Garcia de Tena J (2005) Inflammation, atherosclerosis, and coronary artery disease. N Engl J Med 353:429–430, author reply 429–430
28. Hansson GK (2005) Inflammation, atherosclerosis, and coronary artery disease. N Engl J Med 352:1685–1695
29. Galis ZS, Khatri JJ (2002) Matrix metalloproteinases in vascular remodeling and atherogenesis: the good, the bad, and the ugly. Circ Res 90:251–262
30. Mofidi R, Crotty TB, McCarthy P, Sheehan SJ, Mehigan D, Keaveny TV (2001) Association between plaque instability, angiogenesis and symptomatic carotid occlusive disease. Br J Surg 88:945–950
31. Newby AC (2005) Dual role of matrix metalloproteinases (matrixins) in intimal thickening and atherosclerotic plaque rupture. Physiol Rev 85:1–31
32. Nighoghossian N, Derex L, Douek P (2005) The vulnerable carotid artery plaque: current imaging methods and new perspectives. Stroke 36:2764–2772
33. Cai JM, Hatsukami TS, Ferguson MS, Small R, Polissar NL, Yuan C (2002) Classification of human carotid atherosclerotic lesions with in vivo multicontrast magnetic resonance imaging. Circulation 106:1368–1373
34. Saam T, Ferguson MS, Yarnykh VL, Takaya N, Xu D, Polissar NL, Hatsukami TS, Yuan C (2005) Quantitative evaluation of carotid plaque composition by in vivo MRI. Arterioscler Thromb Vasc Biol 25:234–239
35. Virmani R, Kolodgie FD, Burke AP, Farb A, Schwartz SM (2000) Lessons from sudden coronary death: a comprehensive morphological classification scheme for atherosclerotic lesions. Arterioscler Thromb Vasc Biol 20:1262–1275
36. Hatsukami TS, Ross R, Polissar NL, Yuan C (2000) Visualization of fibrous cap thickness and rupture in human atherosclerotic carotid plaque in vivo with high-resolution magnetic resonance imaging. Circulation 102:959–964
37. Trivedi RA, U-King-Im JM, Graves MJ, Horsley J, Goddard M, Kirkpatrick PJ, Gillard JH (2004) MRI-derived measurements of fibrous-cap and lipid-core thickness: the potential for identifying vulnerable carotid plaques in vivo. Neuroradiology 46: 738–743
38. Cai J, Hatsukami TS, Ferguson MS, Kerwin WS, Saam T, Chu B, Takaya N, Polissar NL, Yuan C (2005) In vivo quantitative measurement of intact fibrous cap and lipid-rich necrotic core size in atherosclerotic carotid plaque: comparison of high-resolution, contrast-enhanced magnetic resonance imaging and histology. Circulation 112:3437–3444

39. Underhill HR, Hatsukami TS, Cai J, Yu W, Demarco JK, Polissar NL, Ota H, Zhao X, Dong L, Oikawa M, Yuan C (2010) A noninvasive imaging approach to assess plaque severity: the carotid atherosclerosis score. AJNR Am J Neuroradiol 31(6):1068–1075
40. Zhao XQ, Dong L, Hatsukami T, Phan BA, Chu B, Moore A, Lane T, Neradilek MB, Polissar N, Monick D, Lee C, Underhill H, Yuan C (2011) MR imaging of carotid plaque composition during lipid-lowering therapy a prospective assessment of effect and time course. JACC Cardiovasc Imaging 4:977–986
41. Spagnoli LG, Mauriello A, Sangiorgi G, Fratoni S, Bonanno E, Schwartz RS, Piepgras DG, Pistolese R, Ippoliti A, Holmes DR Jr (2004) Extracranial thrombotically active carotid plaque as a risk factor for ischemic stroke. JAMA 292:1845–1852
42. Chu B, Ferguson MS, Chen H, Hippe DS, Kerwin WS, Canton G, Yuan C, Hatsukami TS (2009) Magnetic [corrected] resonance imaging [corrected] features of the disruption-prone and the disrupted carotid plaque. JACC Cardiovasc Imaging 2:883–896
43. Qiao Y, Hallock KJ, Hamilton JA (2011) Magnetization transfer magnetic resonance of human atherosclerotic plaques ex vivo detects areas of high protein density. J Cardiovasc Magn Reson 13:73
44. Wang J, Ferguson MS, Balu N, Yuan C, Hatsukami TS, Bornert P (2010) Improved carotid intraplaque hemorrhage imaging using a slab-selective phase-sensitive inversion-recovery (SPI) sequence. Magn Reson Med 64:1332–1340
45. Corti R, Fayad ZA, Fuster V, Worthley SG, Helft G, Chesebro J, Mercuri M, Badimon JJ (2001) Effects of lipid-lowering by simvastatin on human atherosclerotic lesions: a longitudinal study by high-resolution, noninvasive magnetic resonance imaging. Circulation 104:249–252
46. Corti R, Fuster V, Fayad ZA, Worthley SG, Helft G, Smith D, Weinberger J, Wentzel J, Mizsei G, Mercuri M, Badimon JJ (2002) Lipid lowering by simvastatin induces regression of human atherosclerotic lesions: two years' follow-up by high-resolution noninvasive magnetic resonance imaging. Circulation 106:2884–2887
47. Kriszbacher I, Koppan M, Bodis J (2005) Inflammation, atherosclerosis, and coronary artery disease. N Engl J Med 353:429–430, author reply 429–430
48. Kerwin WS, O'Brien KD, Ferguson MS, Polissar N, Hatsukami TS, Yuan C (2006) Inflammation in carotid atherosclerotic plaque: a dynamic contrast-enhanced MR imaging study. Radiology 241:459–468
49. Kooi ME, Cappendijk VC, Cleutjens KB, Kessels AG, Kitslaar PJ, Borgers M, Frederik PM, Daemen MJ, van Engelshoven JM (2003) Accumulation of ultrasmall superparamagnetic particles of iron oxide in human atherosclerotic plaques can be detected by in vivo magnetic resonance imaging. Circulation 107:2453–2458
50. Trivedi RA, U-King-Im JM, Graves MJ, Kirkpatrick PJ, Gillard JH (2004) Noninvasive imaging of carotid plaque inflammation. Neurology 63:187–188
51. Yuan C, Kerwin WS, Ferguson MS, Polissar N, Zhang S, Cai J, Hatsukami TS (2002) Contrast-enhanced high resolution MRI for atherosclerotic carotid artery tissue characterization. J Magn Reson Imaging 15:62–67
52. EMA (2008) International Nonproprietary Name (INN): superparamagnetic iron oxide nanoparticles stabilised with dextran and sodium citrate
53. Schmitz SA, Coupland SE, Gust R, Winterhalter S, Wagner S, Kresse M, Semmler W, Wolf KJ (2000) Superparamagnetic iron oxide-enhanced MRI of atherosclerotic plaques in Watanabe hereditable hyperlipidemic rabbits. Invest Radiol 35:460–471
54. Schmitz SA, Taupitz M, Wagner S, Wolf KJ, Beyersdorff D, Hamm B (2001) Magnetic resonance imaging of atherosclerotic plaques using superparamagnetic iron oxide particles. J Magn Reson Imaging 14:355–361
55. Bulte JW, Brooks RA, Moskowitz BM, Bryant LH Jr, Frank JA (1999) Relaxometry and magnetometry of the MR contrast agent MION-46L. Magn Reson Med 42:379–384
56. Trivedi R, U-King-Im JM, Gillard J (2003) Accumulation of ultrasmall superparamagnetic particles of iron oxide in human atherosclerotic plaque. Circulation 108:e140, author reply e140
57. Trivedi RA, U-King-Im JM, Graves MJ, Cross JJ, Horsley J, Goddard MJ, Skepper JN, Quartey G, Warburton E, Joubert I, Wang L, Kirkpatrick PJ, Brown J, Gillard JH (2004) In vivo detection of macrophages in human carotid atheroma: temporal dependence of ultrasmall superparamagnetic particles of iron oxide-enhanced MRI. Stroke 35:1631–1635
58. Tang TY, Howarth SP, Miller SR, Graves MJ, U-King-Im JM, Li ZY, Walsh SR, Patterson AJ, Kirkpatrick PJ, Warburton EA, Varty K, Gaunt ME, Gillard JH (2008) Correlation of carotid atheromatous plaque inflammation using USPIO-enhanced MR imaging with degree of luminal stenosis. Stroke 39:2144–2147
59. Tang TY, Howarth SP, Li ZY, Miller SR, Graves MJ, U-king-Im JM, Trivedi RA, Walsh SR, Brown AP, Kirkpatrick PJ, Gaunt ME, Gillard JH (2008) Correlation of carotid atheromatous plaque inflammation with biomechanical stress: utility of USPIO enhanced MR imaging and finite element analysis. Atherosclerosis 196:879–887
60. Tang TY, Howarth SP, Miller SR, Graves MJ, Patterson AJ, U-King-Im JM, Li ZY, Walsh SR, Brown AP, Kirkpatrick PJ, Warburton EA, Hayes PD, Varty K, Boyle JR, Gaunt ME, Zalewski A, Gillard JH (2009) The ATHEROMA (atorvastatin therapy: effects on reduction of macrophage activity) study. Evaluation using ultrasmall superparamagnetic iron oxide-enhanced magnetic resonance imaging in carotid disease. J Am Coll Cardiol 53:2039–2050
61. Corti R, Fuster V, Fayad ZA, Worthley SG, Helft G, Chaplin WF, Muntwyler J, Viles-Gonzalez JF, Weinberger J, Smith DA, Mizsei G, Badimon JJ (2005) Effects of aggressive versus conventional lipid-lowering therapy by simvastatin on human atherosclerotic lesions: a prospective, randomized, double-blind trial with high-resolution magnetic resonance imaging. J Am Coll Cardiol 46:106–112
62. Underhill HR, Yuan C, Zhao XQ, Kraiss LW, Parker DL, Saam T, Chu B, Takaya N, Liu F, Polissar NL, Neradilek B, Raichlen JS, Cain VA, Waterton JC, Hamar W, Hatsukami TS (2008) Effect of rosuvastatin therapy on carotid plaque morphology and composition in moderately hypercholesterolemic patients: a high-resolution magnetic resonance imaging trial. Am Heart J 155(584):e1–e8
63. Simonetti OP, Finn JP, White RD, Laub G, Henry DA (1996) "Black blood" T2-weighted inversion-recovery MR imaging of the heart. Radiology 199:49–57
64. Yarnykh VL, Yuan C (2002) T1-insensitive flow suppression using quadruple inversion-recovery. Magn Reson Med 48:899–905
65. Moreno PR, Purushothaman KR, Fuster V, Echeverri D, Truszczynska H, Sharma SK, Badimon JJ, O'Connor WN (2004) Plaque neovascularization is increased in ruptured atherosclerotic lesions of human aorta: implications for plaque vulnerability. Circulation 110:2032–2038
66. Jackson A, O'Connor JP, Parker GJ, Jayson GC (2007) Imaging tumor vascular heterogeneity and angiogenesis using dynamic contrast-enhanced magnetic resonance imaging. Clin Cancer Res 13:3449–3459
67. Aoki S, Aoki K, Ohsawa S, Nakajima H, Kumagai H, Araki T (1999) Dynamic MR imaging of the carotid wall. J Magn Reson Imaging 9:420–427
68. Wasserman BA, Smith WI, Trout HH 3rd, Cannon RO 3rd, Balaban RS, Arai AE (2002) Carotid artery atherosclerosis: in vivo morphologic characterization with gadolinium-enhanced double-oblique MR imaging initial results. Radiology 223:566–573
69. Akella NS, Twieg DB, Mikkelsen T, Hochberg FH, Grossman S, Cloud GA, Nabors LB (2004) Assessment of brain

tumorangiogenesis inhibitors using perfusion magnetic resonance imaging: quality and analysis results of a phase I trial. J Magn Reson Imaging 20:913–922
70. Kerwin W, Hooker A, Spilker M, Vicini P, Ferguson M, Hatsukami T, Yuan C (2003) Quantitative magnetic resonance imaging analysis of neovasculature volume in carotid atherosclerotic plaque. Circulation 107:851–856
71. Briley-Saebo KC, Shaw PX, Mulder WJ, Choi SH, Vucic E, Aguinaldo JG, Witztum JL, Fuster V, Tsimikas S, Fayad ZA (2008) Targeted molecular probes for imaging atherosclerotic lesions with magnetic resonance using antibodies that recognize oxidation-specific epitopes. Circulation 117:3206–3215
72. Chen W, Vucic E, Leupold E, Mulder WJ, Cormode DP, Briley-Saebo KC, Barazza A, Fisher EA, Dathe M, Fayad ZA (2008) Incorporation of an apoE-derived lipopeptide in high-density lipoprotein MRI contrast agents for enhanced imaging of macrophages in atherosclerosis. Contrast Media Mol Imaging 3:233–242
73. Spuentrup E, Botnar RM, Wiethoff AJ, Ibrahim T, Kelle S, Katoh M, Ozgun M, Nagel E, Vymazal J, Graham PB, Gunther RW, Maintz D (2008) MR imaging of thrombi using EP-2104R, a fibrin-specific contrast agent: initial results in patients. Eur Radiol 18:1995–2005
74. Laitinen I, Saraste A, Weidl E, Poethko T, Weber AW, Nekolla SG, Leppanen P, Yla-Herttuala S, Holzlwimmer G, Walch A, Esposito I, Wester HJ, Knuuti J, Schwaiger M (2009) Evaluation of alphavbeta3 integrin-targeted positron emission tomography tracer 18F-galacto-RGD for imaging of vascular inflammation in atherosclerotic mice. Circ Cardiovasc Imaging 2:331–338
75. Mulder WJ, Strijkers GJ, Briley-Saboe KC, Frias JC, Aguinaldo JG, Vucic E, Amirbekian V, Tang C, Chin PT, Nicolay K, Fayad ZA (2007) Molecular imaging of macrophages in atherosclerotic plaques using bimodal PEG-micelles. Magn Reson Med 58:1164–1170
76. Nahrendorf M, Jaffer FA, Kelly KA, Sosnovik DE, Aikawa E, Libby P, Weissleder R (2006) Noninvasive vascular cell adhesion molecule-1 imaging identifies inflammatory activation of cells in atherosclerosis. Circulation 114:1504–1511
77. Lancelot E, Amirbekian V, Brigger I, Raynaud JS, Ballet S, David C, Rousseaux O, Le Greneur S, Port M, Lijnen HR, Bruneval P, Michel JB, Ouimet T, Roques B, Amirbekian S, Hyafil F, Vucic E, Aguinaldo JG, Corot C, Fayad ZA (2008) Evaluation of matrix metalloproteinases in atherosclerosis using a novel noninvasive imaging approach. Arterioscler Thromb Vasc Biol 28:425–432
78. Kaazempur-Mofrad MR, Isasi AG, Younis HF, Chan RC, Hinton DP, Sukhova G, LaMuraglia GM, Lee RT, Kamm RD (2004) Characterization of the atherosclerotic carotid bifurcation using MRI, finite element modeling, and histology. Ann Biomed Eng 32:932–946
79. Baldewsing RA, de Korte CL, Schaar JA, Mastik F, van der Steen AF (2004) Finite element modeling and intravascularultrasound elastography of vulnerable plaques: parameter variation. Ultrasonics 42:723–729
80. Trivedi RA, Li ZY, U-King-Im JM, Graves MJ, Kirkpatrick PJ, Gillard JH (2007) Identifying vulnerable carotid plaques in vivo using high resolution magnetic resonance imaging-based finite element analysis. J Neurosurg 107:536–542
81. Sadat U, Teng Z, Young VE, Li ZY, Gillard JH (2011) Utility of magnetic resonance imaging-based finite element analysis for the biomechanical stress analysis of hemorrhagic and non-hemorrhagic carotid plaques. Circ J 75:884–889
82. Li ZY, Tang TY, Jiang F, Zhang Y, Gillard JH (2011) Reduction in arterial wall strain with aggressive lipid-lowering therapy in patients with carotid artery disease. Circ J 75:1486–1492
83. Moody AR, Murphy RE, Morgan PS, Martel AL, Delay GS, Allder S, MacSweeney ST, Tennant WG, Gladman J, Lowe J, Hunt BJ (2003) Characterization of complicated carotid plaque with magnetic resonance direct thrombus imaging in patients with cerebral ischemia. Circulation 107:3047–3052
84. Bianda N, Di Valentino M, Periat D, Segatto JM, Oberson M, Moccetti M, Sudano I, Santini P, Limoni C, Froio A, Stuber M, Corti R, Gallino A, Wyttenbach R (2012) Progression of human carotid and femoral atherosclerosis: a prospective follow-up study by magnetic resonance vessel wall imaging. Eur Heart J 33:230–237
85. Fayad ZA, Mani V, Woodward M, Kallend D, Abt M, Burgess T, Fuster V, Ballantyne CM, Stein EA, Tardif JC, Rudd JH, Farkouh ME, Tawakol A (2011) Safety and efficacy of dalcetrapib on atherosclerotic disease using novel non-invasive multimodality imaging (dal-PLAQUE): a randomised clinical trial. Lancet 378:1547–1559
86. Yonemura A, Momiyama Y, Fayad ZA, Ayaori M, Ohmori R, Higashi K, Kihara T, Sawada S, Iwamoto N, Ogura M, Taniguchi H, Kusuhara M, Nagata M, Nakamura H, Tamai S, Ohsuzu F (2005) Effect of lipid-lowering therapy with atorvastatin on atherosclerotic aortic plaques detected by noninvasive magnetic resonance imaging. J Am Coll Cardiol 45:733–742
87. Lima JA, Desai MY, Steen H, Warren WP, Gautam S, Lai S (2004) Statin-induced cholesterol lowering and plaque regression after 6 months of magnetic resonance imaging-monitored therapy. Circulation 110:2336–2341
88. Yamaguchi M, Sasaki M, Ohba H, Mori K, Narumi S, Katsura N, Ohura K, Kudo K, Terayama Y (2012) Quantitative assessment of changes in carotid plaques during cilostazol administration using three-dimensional ultrasonography and non-gated magnetic resonance plaque imaging. Neuroradiology 54:939–945
89. Sadat U, Li ZY, Young VE, Graves MJ, Boyle JR, Warburton EA, Varty K, O'Brien E, Gillard JH (2010) Finite element analysis of vulnerable atherosclerotic plaques: a comparison of mechanical stresses within carotid plaques of acute and recently symptomatic patients with carotid artery disease. J Neurol Neurosurg Psychiatry 81:286–289